Environmental Science & Technology

Article

Cite This: Environ. Sci. Technol. XXXX, XXX, XXX−XXX

pubs.acs.org/est

Urban Oxidation Flow Reactor Measurements Reveal Significant Secondary Organic Aerosol Contributions from Volatile Emissions of Emerging Importance

Rishabh U. Shah,[†,‡,¶,§] Matthew M. Coggon,[∥,⊥] Georgios I. Gkatzelis,[∥,⊥] Brian C. McDonald,[∥,⊥] Antonios Tasoglou,[#] Heinz Huber,[#] Jessica Gilman,[∥] Carsten Warneke,[∥,⊥] Allen L. Robinson,[†,‡] and Albert A. Presto*[,†,‡]

[†]Center for Atmospheric Particle Studies, Carnegie Mellon University, Pittsburgh, Pennsylvania 15213, United States

[‡]Mechanical Engineering, Carnegie Mellon University, Pittsburgh, Pennsylvania 15213, United States

[∥]Chemical Sciences Division, National Oceanic and Atmospheric Administration, Earth Systems Research Laboratory, Boulder, Colorado 80305, United States

[⊥]Cooperative Institute for Research in Environmental Sciences, University of Colorado, Boulder, Colorado 80309, United States

[#]R. J. Lee Group Inc., Monroeville, Pennsylvania 15146, United States

Supporting Information

ABSTRACT: Mobile sampling studies have revealed enhanced levels of secondary organic aerosol (SOA) in source-rich urban environments. While these enhancements can be from rapidly reacting vehicular emissions, it was recently hypothesized that nontraditional emissions (volatile chemical products and upstream emissions) are emerging as important sources of urban SOA. We tested this hypothesis by using gas and aerosol mass spectrometry coupled with an oxidation flow reactor (OFR) to characterize pollution levels and SOA potentials in environments influenced by traditional emissions (vehicular, biogenic), and nontraditional emissions (e.g., paint fumes). We used two SOA models to assess contributions of vehicular and biogenic emissions to our observed SOA. The largest gap between observed and modeled SOA potential occurs in the morning-time urban street canyon environment, for which our model can only explain half of our observation. Contributions from VCP emissions (e.g., personal care products) are highest in this environment, suggesting that VCPs are an important missing source of precursors that would close the gap between modeled and observed SOA potential. Targeted OFR oxidation of nontraditional emissions shows that these emissions have SOA potentials that are similar, if not larger, compared to vehicular emissions. Laboratory experiments reveal large differences in SOA potentials of VCPs, implying the need for further characterization of these nontraditional emissions.

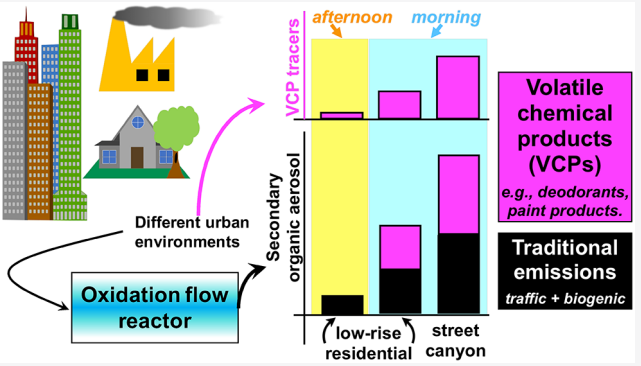

INTRODUCTION

Atmospheric particulate matter (PM) with diameter smaller than 2.5 μm ($PM_{2.5}$) has deleterious effects on human health,[1] and it also affects the Earth's climate.[2] Numerous ambient measurements have shown that organic aerosol (OA) comprises a dominant fraction of PM mass in most regions of the atmosphere, including urban areas.[3−5] After emission, primary OA and coemitted reactive organic gases evolve in the atmosphere, resulting in formation of secondary OA (SOA), which is a dominant contributor to global OA mass.[4,6]

Atmospheric chemistry models often underpredict urban SOA formation, likely because the emission inventories used by these models are missing large sources of rapidly reacting SOA precursors.[7−10] Recent studies have proposed that organic gas emissions from volatile chemical products (VCPs; e.g., pigment coatings, personal care products) are an important source of urban SOA precursors, rivaling those from traditional sources, such as gasoline and diesel vehicles.[9,11] Radiocarbon dating of urban aerosol has also implied that an important source of urban SOA is volatile organic emissions of petrochemical origin, that is, vehicles and VCPs.[12,13] While some recent studies have studied the SOA potential of single VCP compounds,[14] the hypothesis that VCPs are significant urban SOA precursors has not yet been experimentally tested. It is, however, likely that these VCP

Received: October 30, 2019
Revised: December 18, 2019
Accepted: December 18, 2019
Published: December 18, 2019

DOI: 10.1021/acs.est.9b06531
Environ. Sci. Technol. XXXX, XXX, XXX−XXX

constituents may have significant SOA mass yields under atmospherically relevant conditions. It is thus critical to understand how VCP emissions contribute to urban SOA formation. Aside from VCPs, upstream organic emissions (e.g., oil and natural gas extraction and enrichment, refineries, tar sands exploration, etc.) are significantly underpredicted in the National Emission Inventory, and their role in atmospheric chemistry is thus poorly constrained.[15,16] One reason for this is that these large industrial facilities contain several different subunits and thus have fugitive emissions from several points along the process that are difficult to quantify.[17,18] A mass balance of organic compounds through the U.S. petrochemical industry revealed that of the 17 Tg of organic gas emissions in 2012, only 5 Tg were from gasoline and diesel exhaust, with upstream emissions and VCPs contributing roughly equally to the remaining 12 Tg.[9] While particulate matter levels are regulated both at points of emission[19] and in ambient air,[20] regulations on these nonmobile and upstream sources of reactive organic gases are less stringent. Further, these organic gases are regulated with attention to their potential to form tropospheric O_3, and less attention is paid to their SOA potential. Identification of organic gases that are efficient SOA precursors can thus aid in reducing discrepancies between observed and modeled SOA, and better constrain the annual SOA budget at the national scale.

At the intraurban scale, recent high-spatial-resolution measurements have shown spatial variabilities in VCP tracers and SOA, with above-background enhancements in city centers and industrial regions.[5,21−24] This suggests that different intraurban environments have different extents/rates of SOA production because of greater emissions. In addition to spatial variabilities, diurnal patterns of observed SOA are also consistent with those of precursor emissions from vehicles and VCPs.[21,23] It is thus reasonable to expect that rapidly reacting SOA precursors from VCPs influence these observed spatial and temporal variabilities in intraurban SOA.

In this study, we investigate differences in SOA formation potentials across different urban environments using a compact oxidation flow reactor (OFR) deployed in a mobile laboratory. We show results of OFR sampling in typical urban environments, and also in environments that are more heavily influenced by nontraditional emissions. We also present results of laboratory experiments that underscore the magnitudes and source-dependent variabilities in SOA potentials of VCPs. The objective of this study is to empirically test two hypotheses in densely populated urban environments: (a) nontraditional emissions, such as VCPs are an important source of rapidly reacting SOA precursors and (b) intraurban variability in SOA potential occurs due to traditional (vehicles, biogenic) and nontraditional sources similarly.

METHODS

We performed measurements in/around Pittsburgh, PA and New York City, NY metro areas. We oxidized ambient air in our oxidation flow reactor (OFR), measured the amount of SOA produced in the OFR, and used these measurements to infer the SOA potential in different urban environments. Our primary goal was to distinguish different sources of SOA and to assess the importance of traditional and nontraditional SOA precursor sources. Because anthropogenic emissions are variable both spatially and temporally, our use of the term "environment" is not just defined in space (e.g., street canyon), but also in time (e.g., morning-time street canyon). We visited five environments: (1) morning-time urban street canyon, (2) morning-time urban low-rise, (3) afternoon-time urban low-rise, (4) industrial coke production plume, and (5) construction site. The air quality in the first three environments is heavily influenced by vehicular emissions, and thus, we collectively refer to them as typical urban environments. The industrial facility is the largest metallurgical coke manufacturing facility in the U.S. and is a well-documented strong source of $PM_{2.5}$ (900 tons per year[25,26]), and hazardous organic gases.[27] At the construction site, spray-painting and sealcoating activities were a strong source of VCP emissions. We collectively refer to the industrial and construction sites as nontypical urban environments.

We also reproduced the VCP-influenced plumes in the laboratory using a select few VCPs (e.g., personal care products) and characterized variabilities in SOA potential across different VCP types.

Outdoor Sampling Locations and Instrumentation. We performed morning-time urban street canyon measurements in downtown Pittsburgh, PA (majority buildings >20 m tall), and in Harlem, New York City, NY (majority buildings <20 m tall) in July 2018. We performed coke production plume measurements in Clairton, PA in October 2018. Pittsburgh and Harlem measurements were performed in the morning (8 AM to 11 AM). Measurements in Harlem were also done in the afternoon (1 PM to 4 PM). Measurements in Clairton were done from 7 AM to 9 AM. Sampling locations and other details about the environments are shown in the SI.

We measured aerosol mass and chemical composition with a high-resolution time-of-flight aerosol mass spectrometer (AMS; 1 min sampling; Aerodyne Research Inc.), and aerosol size distributions with a scanning mobility particle sizer (SMPS; 3 min sampling; TSI Inc.). These instruments were deployed in the Carnegie Mellon University (CMU) mobile laboratory. Every 10 min, the aerosol sampling source was alternated between the OFR and a bypass (ambient) line to measure real-time enhancement of aerosol mass upon processing in the OFR.

Ambient organic gases were measured by high-resolution proton-transfer-reaction time-of-flight mass spectrometers (PTRMS) external to the CMU van. With the exception of the industrial site in Clairton, we used the customized "NOAA PTR-ToF-MS"[23,28] aboard the NOAA Chemical Sciences Division mobile laboratory.[23] In Clairton, we used a commercial PTR-ToF-4000 (Ionicon Analytik). A list of species measured and analyzed by these instruments is provided in the SI.

At the construction site (Oakland neighborhood, Pittsburgh; Figure S10), we performed mobile OFR sampling of VCP fumes. To capture rapid variability, the AMS and SMPS only sampled through the OFR (lamps held at steady voltage), with the AMS sampling every 20 s.

Oxidation Flow Reactor (OFR). We used a custom-built, 3.6 L cylindrical aluminum OFR, operated at a nominal flow residence time (τ) of 1 min. In the OFR, hydroxyl radical (OH) is formed upon controlled photolysis of oxygen and humidity present in the inflowing air (details in SI). We injected CO at the reactor inlet (nominally 3 ppm of CO after mixing with ambient air), and used its decay to estimate real-time OH concentrations in the OFR.[29,30] This approach inherently accounts for any effect of varying ambient OH reactivity (e.g., from NO_x) on OH concentrations inside the OFR. We also calibrated OH concentrations offline, and

DOI: 10.1021/acs.est.9b06531
Environ. Sci. Technol. XXXX, XXX, XXX−XXX

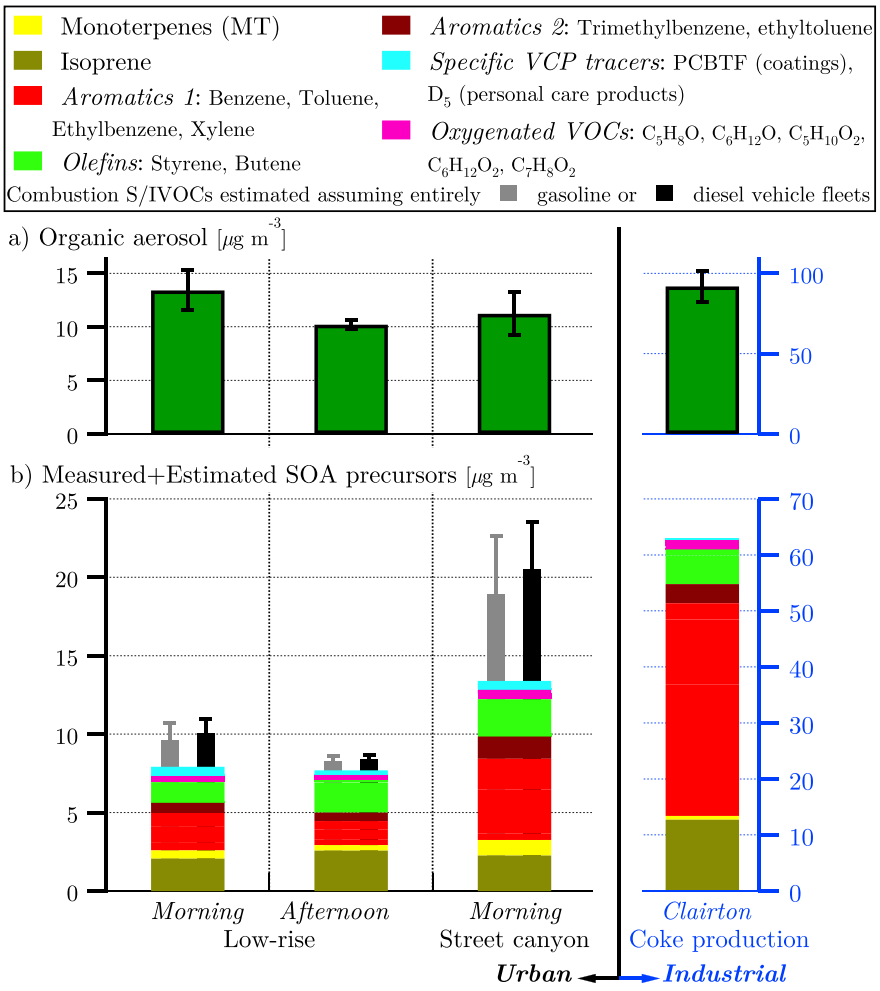

Figure 1. (a) OA and (b) SOA precursors in urban (left axes) and industrial (right axes) environments. Error bars on OA data are 1 σ. S/IVOCs from vehicles are estimated using published emission factor ratios of S/IVOCs-to-OA for gasoline and diesel vehicle emissions.[46−48] Error bars on S/IVOCs indicate bounds of estimated combustion S/IVOCs, arising from the uncertainties in the IVOC-HOA relationships of Zhao et al.[46,47] Because of the lack of information about chemical composition of coke production emissions, we did not estimate S/IVOCs for the industrial site. Due to lack of resolution about isomers, we only show the chemical formulas of the oxygenated VOCs.

verified our calibrations against the Peng et al.[31] model (Figure S2). We systematically varied OH exposures (OH_{exp} = [OH] × τ) by stepping the voltage supplied to the ultraviolet lamps. OH_{exp} was then converted to an equivalent atmospheric age assuming a daily average OH concentration of 1.5 × 10^6 molecules cm^{-3}.[32] In a typical OFR experiment, we stepped through 4−5 different lamp voltage settings, including a "dark" setting (i.e., lamps off). We used the ratio of ambient OA to that measured through dark reactor (typically 1.2) to account for any particle mass lost to reactor surfaces. We also evaluated other loss mechanisms in our OFR, such as photolysis, excessive fragmentation, etc., using previously published models (details in SI).[31,33]

Data Analysis. AMS data were processed using SQUIRREL 1.57I and PIKA 1.16I routines in Igor Pro.[34] Data were corrected for transmission and ionization efficiencies of the AMS, and composition-dependent collection efficiency.[35] Hydrocarbon-like OA (HOA) from vehicles was estimated as a linear combination of select high-resolution tracer fragments in the OA mass spectra (C_4H_9, C_4H_7, and CO_2^+ at m/z 57, 55, 44, respectively), similar to approaches reported previously[29,36,37] (details in Figure S11).

Estimating Unmeasured SOA Precursors. Atmospheric organic mixtures consist of compounds that are present in a single phase (particles and gases), and compounds that are in two-phase equilibria. The two-dimensional volatility basis set (2D-VBS)[38,39] framework describes the mass distribution of these organic mixtures using volatility bins, with nonvolatile and low-volatility bins (N- and LVOCs) containing particle-phase mass, semivolatile bins having a mixture of particle- and gas-phase compounds (SVOCs), and bins of higher volatilities (intermediate-volatility organic compounds (IVOCs), and VOCs) containing gas-phase mass. The OA measured by the AMS thus consists of all N- and LVOCs, and particle-phase SVOCs. Gases measured by the PTRMS are mostly VOCs, since it is challenging to measure gas-phase S/IVOCs with this technique.[40−42] However, these S/IVOCs are important SOA precursors[43,44] and improve closure between modeled and observed SOA.[8,30,45]

Zhao et al.[46,47] showed that the IVOC-to-HOA ratios of gasoline and diesel vehicle emissions are 6.2 ± 4.4 and 8.0 ± 3.6, respectively (integrated over the cold-start unified drive cycle). Recently, Lu et al.[48] showed a relationship between SVOC and IVOC mass fractions across a variety of emission sources including gasoline and diesel vehicles. We use the

DOI: 10.1021/acs.est.9b06531
Environ. Sci. Technol. XXXX, XXX, XXX−XXX

IVOC-to-HOA ratios of Zhao et al.,[46,47] and the SVOC-IVOC relationship of Lu et al.[48] to estimate combustion S/IVOCs from vehicular emissions in our typical urban environments.

SOA Prediction. We predicted SOA from measured and estimated ambient precursor concentrations and source types at the typical urban environments and the coke manufacturing site, though we did not account for any S/IVOCs for the latter. While emission factors have been published on individual S/IVOCs,[18] we are not aware of studies that have published the total (speciated + unspeciated) S/IVOC emissions in coke production emissions.

We used speciated and source-based approaches to predict SOA production in the OFR. In the speciated approach, we used the individual precursor concentrations (from Figure 1), their respective reaction rate constants with OH, and previously characterized SOA yields from literature (details in Table S1). We used high-NO_x SOA yields if available, thereby invoking the assumption of high-NO_x regimes in our typical urban environments. For combustion S/IVOCs, we used the rate constant used previously to represent reactivity of unresolved complex mixtures of organic gases in OFR conditions,[49] and the *n*-alkane surrogate yields for gasoline and diesel emissions reported by Jathar et al.[50] We calculated SOA formation at 2 days of OH_{exp}, since this is the time scale for peak SOA formation in the OFR.[29,45,51]

The source-based approach follows Saha et al.[29] Here, we consider vehicular and biogenic emissions as two important SOA precursor groups in typical urban environments. We considered ambient monoterpene and isoprene measurements collectively as "biogenic" (while using their individual yields from the OFR measurements of Lambe et al.[52]), and HOA as a metric for vehicular emissions. We used the peak OA enhancement ratio observed inside a highway tunnel by Tkacik et al.[51] as the maximum possible SOA that can be achieved from OFR-oxidation of air influenced by vehicular emissions. Since Lambe et al.[52] and Tkacik et al.[51] reported OFR-based SOA measurements, these parametrizations also account for multigenerational chemistry that may occur under the high OH conditions in the OFR. We only estimated biogenic SOA for the coke manufacturing site.

RESULTS AND DISCUSSION

Ambient Organic Concentrations in Typical Urban Environments. In Figure 1, we present ambient OA and SOA precursor concentrations in typical urban and industrial environments where we performed stationary sampling. We grouped important SOA precursors consistently with how they are typically grouped in chemical transport models.[53]

Ambient OA in the typical urban environments are similar to each other (10−13 $\mu g\ m^{-3}$) and to previous urban measurements.[5,54] We estimated HOA concentrations of 0.8, 0.3, and 0.1 $\mu g\ m^{-3}$ in the street canyon, morning-time low-rise, and afternoon-time low-rise urban environments, respectively. These values are consistent with those reported previously for high- and low-source urban environments in the U.S.[21,22,55,56] OA and precursor levels were much higher (90 $\mu g\ m^{-3}$ OA, 60 $\mu g\ m^{-3}$ precursors) at the industrial site, because we sampled directly downwind of the Clairton coke works plant during a strong meteorological inversion, which can trap the pollutants near ground level.[57−60] These gas- and particle-phase measurements are consistent with previous fenceline measurements performed downwind of this industrial facility.[25,61]

Figure 1 also shows estimated S/IVOCs emitted from gasoline and diesel vehicles in the typical urban environments. Among these environments, the largest amount of observed + estimated precursors are in the street canyon (20.1 ± 3.7 $\mu g\ m^{-3}$). This point is reinforced later in Figure 2c, in which the

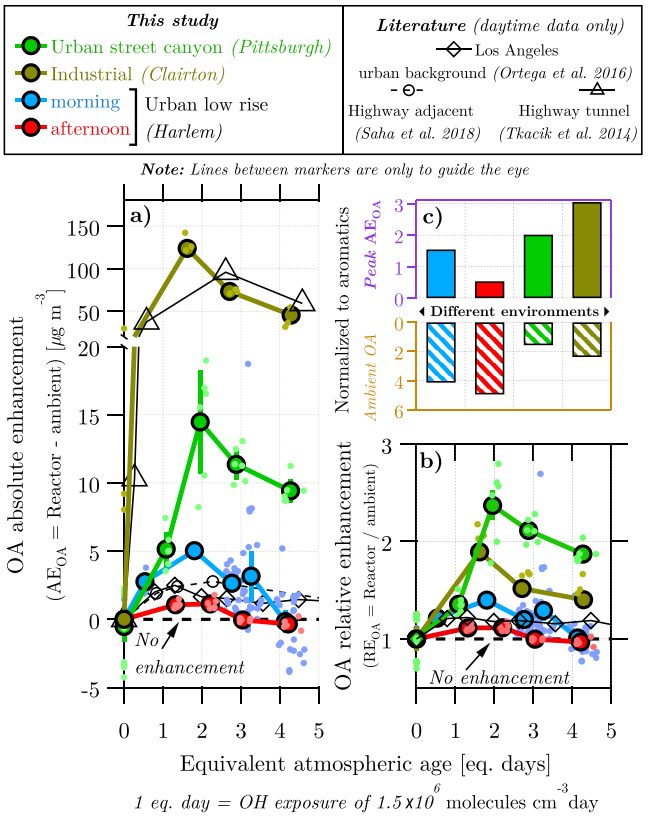

Figure 2. OA mass enhancements in different environments, reported as (a) absolute (AE_{OA} = OFR − ambient) and (b) relative (RE_{OA} = OFR/ambient) enhancements versus integrated OH exposure in the OFR. OH exposure is converted to equivalent atmospheric age assuming daily average ambient [OH] = 1.5 × 10^6 molecules cm^{-3}. Lighter dots are individual data; circles are binned averages. For comparison, literature data show results of similar OFR experiments performed in typical urban environments. In panel c, the ambient OA (hatched bars, reversed) and peak AE_{OA} (solid bars) in each environment are normalized to the amount of ambient aromatics. The purpose of this is simply to relate the SOA potential to the unreacted organic gases shown in Figure 1, and thus we use total concentrations of aromatics as a proxy for all SOA precursors. Each bar represents a different environment and is colored accordingly.

hatched bars represent the ratios of OA to precursors in the different environments. This ratio is lowest for the urban street canyon environment, indicating highest amount of unreacted precursors relative to ambient OA (in other words, SOA potential).

Of the three typical urban environments, the street canyon has the highest concentrations of aromatics. This is expected because of high levels of traffic and reduced dispersion in the street canyon. However, Figure 1 also shows more monoterpenes (MTs) in the street canyon than in the urban low-rise environments and the industrial environment, despite the latter having a denser tree cover (see Figures S7−S9). The ratio of monoterpenes to isoprene is highest in the densely populated street canyon, followed by the urban low-rise environments, and then the sparsely populated semirural

DOI: 10.1021/acs.est.9b06531
Environ. Sci. Technol. XXXX, XXX, XXX−XXX

industrial area. Since we sampled in the typical urban environments within a month, these intraurban MT/isoprene variabilities are likely due more to local emissions than to seasonal variations of natural MT emissions. While MTs (e.g., α-pinene) and isoprene are the dominant SOA precursors emitted from the biosphere, some reactive MTs are also used as ingredients in VCPs (e.g., limonene, which reacts with OH 4× faster than α-pinene,[62] is used in household cleaning and personal care products[63]). Thus, compared to the exclusively naturally emitted isoprene, MTs can exhibit larger spatial and temporal variability across urban environments,[64] with larger contributions in areas with high population density.

Similar to MTs, concentrations of VCP tracers are highest in the street canyon, followed by the low-rise environments. PCBTF (parachlorobenzotriflouride) is commonly used as a solvent in paints, coatings, inks, etc.[65] D_5 (decamethylcyclopentasiloxane) is widely used in consumer products, such as deodorants, and commonly observed in urban air, especially populous areas.[23] Oxygenated VOCs, a potentially important class of VCP-emitted precursors,[9,66,67] are also higher in the urban street canyon compared to the low-rise environments, as shown in Figure 1. These pieces of evidence all suggest that the influence of VCP emissions was strongest in the street canyon, followed by the morning-time urban low-rise environment.

Measured SOA Potentials in Typical Urban Environments. Figure 2a and b shows the absolute and relative OA mass enhancements (AE_{OA} = OFR − ambient, RE_{OA} = OFR/ambient, respectively) with increasing equivalent (equiv) atmospheric age in the OFR for different environments. Overall, in all environments, the mass enhancement increases with increasing equivalent age, peaking at 1.5 to 2 equiv days, and then decreases with additional aging, consistent with previous OFR results.[29,45,49,68] This trend occurs because at shorter ages (<2−3 days), functionalization and condensation mechanisms dominate the chemical processing, while at longer ages (>3 days) fragmentation mechanisms are more important.[29,45,51] Figure 2c shows the ratios of ambient OA and peak AE_{OA}, respectively, to the unreacted aromatics measured in the different environments. Aromatics are important anthropogenic SOA precursors.[8,69] Hence, ratios with aromatics are meant to relate the SOA potentials in different environments to the amount of traditional urban precursors shown in Figure 1.

We will focus on the three typical urban environments in this section and discuss the Clairton coke works plume results in a later section. Among the typical urban environments, the street canyon has the highest SOA formation, with the largest peaks in both RE_{OA} (2.5 × ambient OA), and AE_{OA} (15 $\mu g\ m^{-3}$). In the urban low-rise, peak AE_{OA} of 5 and 1 $\mu g\ m^{-3}$ are observed in the morning and afternoon, respectively, corresponding to RE_{OA} of 1.5 and 1.1 × ambient OA. This morning-afternoon shift in SOA potential is consistent with the findings of Ortega et al.,[45] and indicates increased morning-time emissions of precursors (from vehicles and VCPs[23]). As proposed by Ortega et al.,[45] this phenomenon occurs because of rapid oxidation of these morning-time emissions, reducing the SOA potential in the afternoon. This phenomenon is more clearly illustrated in Figure 2c. The ratios of ambient OA and peak SOA to aromatics complement each other in describing the SOA potential of an environment. Simply put, a smaller ratio of ambient OA to aromatics indicates a larger SOA potential, and thus would be accompanied by more SOA per unit aromatics in the OFR. We observe this trend for all three typical urban environments (all of which have similar ambient OA levels). The ambient OA/aromatics ratio is lowest in the street canyon, suggesting that there is a large pool of unreacted precursors in that environment. As a result, the SOA potential should be (and is) highest in the street canyon. Further, from morning to afternoon, this ambient reactive pool is either consumed or advected away, resulting in lower SOA potential in the afternoon.[45]

While aromatics are an indicator of anthropogenic emissions of SOA precursors, there are other important precursors emitted in typical urban environments, especially in the morning, for example, S/IVOCs from vehicles.[8,44] Non-vehicular sources likely also contribute substantially to these S/IVOCs. Two possible nonvehicular S/IVOC sources could be cooking emissions[8] and VCPs.[9,11] While cooking emissions have been shown to substantially impact urban OA,[5,21,22,70,71] several recent studies suggest that oxidation of cooking emissions forms negligible SOA,[72−74] although contrary findings also exist.[75] Nonetheless, the diurnal profiles of cooking emissions peak at noontime.[21] Thus, if cooking emitted important SOA precursors, these would have a stronger effect on urban SOA during lunch time. However, this effect is observed neither here nor in previous observations.[45]

VCP emissions from personal care products are higher in areas of higher population density,[23] and their diurnal profiles peak in the morning,[23] which coincides with the increased morning-time SOA potential observed here. We thus hypothesize that in addition to traditional sources, VCP emissions also have an important influence on our observed SOA potentials across typical urban environments. This hypothesis is not only consistent with the findings presented here, but would also support previously reported findings of higher SOA in urban street canyons.[21,22] We further investigate this hypothesis in the next section.

Predicted SOA Potentials in Typical Urban Environments. In this section, we compare SOA potential observed in the OFR to that predicted using our speciated and source-based approaches. Results of SOA predictions are shown in Figure 3 as solid bars (speciated approach) and hatched bars (source-based approach).

The speciated approach predicts less SOA potential than the source-based approach. This is likely because of several reasons. First, SOA yields derived from environmental chamber experiments are often underpredicted due to wall effects.[76] Second, while SOA yields have been shown to depend on NO_x levels,[77] literature yields for precursors are often classified into two NO_x conditions (low NO_x and high NO_x). Since we used high NO_x yields in our calculations, SOA predicted using this approach is conservative. Third, the PTRMS misses important SOA precursors, such as alkanes, cycloalkanes, etc., that could also contribute to SOA. Fourth, at the OH concentrations in the OFR, multigenerational chemistry can also affect the SOA yield. Fifth, following Jathar et al.[50] and Drozd et al.,[78] we treat all S/IVOCs as either *n*-tridecane (gasoline) or *n*-pentadecane (diesel), thereby missing the multicomponent complexities of the actual vehicle emissions. Instead of relying on chamber-derived yields, the source-based approach relies on OFR-measured SOA enhancement ratios (RE_{OA}). As a result, these alternate yields are not only not influenced by wall effects, they also implicitly account for influences of NO_x and multigenerational chemistry at OFR-relevant OH levels. Further, since Tkacik et al.[51] performed

DOI: 10.1021/acs.est.9b06531
Environ. Sci. Technol. XXXX, XXX, XXX−XXX

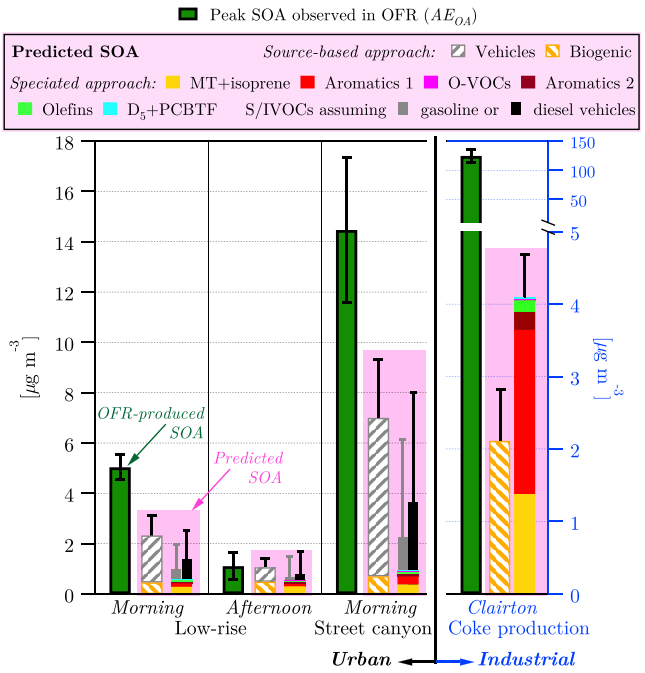

Figure 3. Measured and predicted SOA in different environments at 2 equiv days of OH_{exp}. The peak absolute OA enhancements (AE_{OA}) measured in the OFR (from Figure 2) are shown as green bars, with error bars indicating propagated variations of individual ambient and reactor OA data. SOA predictions are shown within pink tints. Source-based (hatched bars) and speciated (solid bars) approaches are used separately to predict SOA. The speciated approach was run separately to account for different S/IVOC-OA relations for gasoline (gray) and diesel (black) emissions, as shown in Figure 1. Error bars on the speciated approach results indicate propagated uncertainties in gasoline and diesel S/IVOC-HOA relations, uncertainties in literature yields, and variations in gas-phase measurements. Errors on hatched bars indicate bounds calculated by choosing minimum and maximum yields reported in relevant OFR literature.

OFR-oxidation of air inside a highway tunnel, their RE_{OA} is representative of vehicular emissions. For the purposes of this study, the speciated approach should thus be thought of as a lower bound of the predicted SOA potential.

Overall, both our SOA prediction approaches follow the same trend as the OFR-measured peak AE_{OA}: the largest SOA potential occurs in the street canyon, followed by morning-time urban low-rise, and then the afternoon-time urban low-rise environment. Further, both approaches are able to explain the OFR-measured SOA potential for the afternoon urban low-rise environment (within 7%). However, both approaches underestimate SOA potential in the other two environments. For example, the source-based approach is on average unable to explain 7.5 and 2.7 $\mu g\ m^{-3}$ SOA potential in the street canyon and morning-time urban low-rise. It is unable to explain nearly 50% of the observed SOA in both these urban environments. This suggests that there are important sources of SOA precursors in addition to traffic and biogenics in street canyon and morning-time urban low-rise environments.

Figure 3 shows that the predicted SOA from vehicular S/IVOCs is relatively insensitive to the vehicle fleet composition (i.e., gasoline versus diesel vehicles). Assuming a pure diesel fleet (instead of pure gasoline) for the street canyon environment only increases the predicted SOA by 0.7 $\mu g\ m^{-3}$, still preserving the gap of about 7 $\mu g\ m^{-3}$ between observed and predicted SOA. In addition to fuel type, vehicle operating conditions can also impact the S/IVOC emissions. Zhao et al.[47] showed that cold-start emissions have a higher IVOC/OA ratio. However, the source-apportionment results of Gu et al.[22] and Sun et al.[54] both showed traffic emissions starting to peak at 6 AM in Pittsburgh and New York, respectively. Since our urban morning measurements begin after 8 AM local time, cold starts are unlikely to explain the additional observed SOA in the morning. Additionally, many vehicles arriving at the street canyon environment in Pittsburgh first traveled on a highway and were thus presumably warmed up.

Zhao et al.[44] measured ambient IVOCs and aromatics in the Los Angeles urban background and found that they had negligible weekend/weekday variations. This suggested that there is an important source of S/IVOCs in urban areas that has little weekend/weekday dependence. Domestic gasoline vehicles and VCPs (e.g., personal care products) fit this description. Our measurements suggest that influence of VCP emissions was strongest in the street canyon, followed by the morning-time low-rise environment. We, therefore, hypothesize that the unexplained SOA in our typical urban environments is the result of oxidation of noncombustion and nonbiogenic precursors, including S/IVOCs and oxygenated VOCs emitted from VCPs. To close the SOA mass balance in these environments would require 15−20 $\mu g\ m^{-3}$ of unreacted, C_{15}-equivalent S/IVOCs (or other VOCs not measured by the PTRMS) to be present in the street canyon environment (5−7 $\mu g\ m^{-3}$ in the urban low-rise). Following our hypothesis, the amount of SOA potential from VCPs (8 $\mu g\ m^{-3}$) is larger than that from vehicles (6.3 $\mu g\ m^{-3}$) in the street canyon environment. The ratio of SOA potentials of VCPs to that of vehicles is 1.3. This VCP/vehicle ratio of SOA potential is comparable with the estimate of McDonald et al.[9] for Los Angeles urban background (ratio of SOA potential of consumer VCPs to fossil fuel combustion emissions = 1.4). Our findings therefore empirically support the hypothesis of McDonald et al.,[9] that compared to vehicles, VCPs contribute an equal if not great amount of SOA relative to vehicular emissions.

Our analysis attributes aromatics and MTs to vehicles and biogenic sources, respectively. By extension, the SOA that was predicted from these precursors using the speciated approach was attributed to "vehicle" and "biogenic" origin, and only the difference between this predicted SOA and the OFR-observed SOA was attributed to VCPs. However, it is very likely that a fraction of the ambient aromatics and monoterpenes were VCP-emitted,[23] and we therefore misattributed them.

SOA Potentials in Environments Influenced by Nontraditional Emissions. In the previous section, we compared our OFR-measured SOA using speciated and source-based modeling of traditional sources, and attributed the unexplained SOA to nontraditional sources, such as VCPs. While we lumped all VCPs into a single surrogate compound (C_{15}), this is a broad generalization because different VCPs have widely varying chemical compositions and thus different SOA yields. Similarly, other relatively less characterized sources of SOA precursors also likely have varying chemical compositions. For instance, the industrial coke production plume in Clairton had a largely different mixture of organic species (with much higher aromatic concentrations) relative to typical urban environments (Figure 1). In this section, we first discuss OFR-produced SOA ∼ 3 km downwind of this industrial coke manufacturing site. Next, we discuss results of

DOI: 10.1021/acs.est.9b06531
Environ. Sci. Technol. XXXX, XXX, XXX−XXX

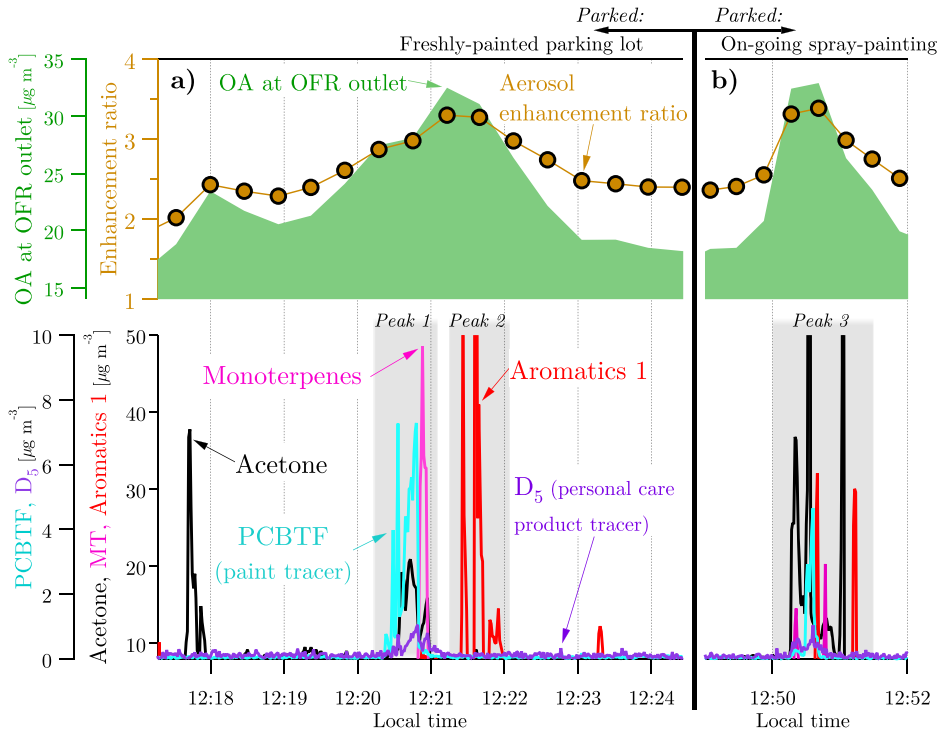

Figure 4. Time series of quasi-mobile OFR sampling performed near two active construction sites in Pittsburgh. Gas-phase measurements (plotted as lines) are at 1 s resolution, while aerosol measurements (plotted as shaded area and markers) are at 20 s resolution. Data are shown for when sampling vans were parked adjacent to VCP sources, that is, (a) a freshly seal-coated parking lot and (b) ongoing spray-painting activity. Gas measurements are at OFR inlet, while particle−phase measurements are at OFR outlet. Aerosol data timestamps are adjusted to account for nominal residence time through OFR and plumbing.

mobile sampling at the construction facility in Pittsburgh, where the air quality was largely influenced by VCP emissions. Lastly, we present results of laboratory experiments that underscore the variability of SOA yields from a select few VCPs.

Industrial Coke Production Site: A Source of Upstream Emissions. Concentrations of gas- and particle-phase organics in the industrial coke production plume are almost 8 times higher than in the typical urban environments (Figure 1). These high concentrations are due to a combination of high emissions and trapping of the plume under a meteorological inversion.[57−60] The chemical composition of this plume was also largely different than in typical urban environments. Aromatics, such as benzene and styrene, contributed nearly two-thirds of the measured organic gases, with benzene contributing 56% of the aromatics (benzene contributed 15% of aromatics in the typical urban environments).

In addition to posing a direct health threat to the downwind suburban vicinity, the organic gases in this industrial plume are also important SOA precursors. As seen in Figure 2, the largest AE_{OA}, 125 $\mu g\ m^{-3}$, is observed in this plume. The AE_{OA} values observed here are similar to those observed in a highway tunnel by Tkacik et al.[51] The AE_{OA} in both these environments are comparable and can be thought of as SOA potentials in insufficiently ventilated areas with high concentrations of SOA precursors.

Despite high pollutant concentrations, the peak RE_{OA} in the industrial environment is lower than that observed in the street canyon. However, the SOA potential of this industrial plume, if inferred from the ratio of peak AE_{OA} to aromatics (Figure 2c), is higher than the street canyon. This is because the chemical composition of the industrial plume is different than that in the street canyon, with a larger aromatics fraction. During coke production, volatile material is removed from coal via destructive distillation in the absence of oxygen. These emissions would thus be expected to span a wide range of volatilities. The nonvolatile and low-volatility organics cool and condense upon emission, resulting in the high OA levels observed downwind. While volatile organics, such as single-ring aromatics are measured by the PTRMS, S/IVOCs are likely also emitted but are not measured by our methods. This is evidenced by the large (120 $\mu g\ m^{-3}$) gap between the SOA measured in the OFR, and that predicted by the speciated approach. Approximately 300−500 $\mu g\ m^{-3}$ of C_{15}-equivalent S/IVOCs would need to be present in this plume to close this SOA gap. The fenceline measurements of Weitkamp et al.[25] showed that this coke manufacturing facility emits on average 420 Mg of primary organic aerosol annually. Using this as a scaling factor, our results show that this industrial site emits 1400−2300 Mg of S/IVOCs, which, via SOA formation, result in an annual average of 580 Mg additional OA (i.e., more than twice the primary OA). While McDonald et al.[9] showed that the magnitude of upstream emissions is significant at the national level, our findings complement this by emphasizing their SOA contribution.

Urban Construction Site: A Source of VCPs. In this section, we show that in a ∼250 m vicinity of a construction site, potential aerosol mass has a variability of over 10 $\mu g\ m^{-3}$, and this variability is strongly influenced by VCP emissions associated with construction activity. Figure 4 shows time series of measured ambient organic gases and OFR-produced SOA around two parts of a construction site in Pittsburgh. The AMS data shown are only products exiting the OFR, while the gas data are ambient concentrations measured adjacent to the

DOI: 10.1021/acs.est.9b06531
Environ. Sci. Technol. XXXX, XXX, XXX−XXX

OFR and can, thus, be thought of as concentrations entering the OFR. An expanded version of this time series is shown in Figure S15, including measurements made sufficiently distant/upwind from the construction sites to be used as background reference. At this upwind location, RE_{OA} was 1.8 ± 0.1, similar to typical urban low-rise environments (Figure 2).

During the first few minutes (until 12:24) of the time series, measurements were made 10 m away from a freshly seal-coated parking lot (4a). At this location, two sets of sharp peaks (labeled as peak 1 and peak 2) occur in the time series of all gases shown in the figure ($\Delta D_5 > 5$ μg m^{-3}, $\Delta PCBTF > 3$ μg m^{-3}, and ΔMT, Δacetone, Δaromatics > 20 μg m^{-3}). These peaks are accompanied by a 10 μg m^{-3} increment in SOA formed in the OFR. Figure 4b shows measurements collected 50 m downwind of another part of the construction site (~250 m from the sealcoated parking lot) during active spray painting. Once again, sharp peaks in D_5, PCBTF, aromatics, and acetone (labeled as peak 3) were accompanied by an AE_{OA} of 10 μg m^{-3}.

Sharp peaks in organic vapors likely indicate the sampling inlet going in and out of the emissions plume. The resulting absolute SOA enhancement increases by over 10 μg m^{-3} at both the parking lot and the spray painting site, and relative enhancement doubles in response to the VCP spikes. While driving away from the seal-coated parking lot, the time series of all gases and OFR-output OA fall to "baseline" levels, suggesting that the SOA increments were caused by the spikes in organic gases.

While the increments in OFR-produced SOA are similar at the parking lot and the spray-painting sites, the composition of the emissions are different. At the parking lot, two distinct sets of gas peaks occur ~1 min apart: peak 1 includes MT, D_5, and PCBTF, while peak 2 is aromatics. PCBTF is used as a tracer for paint products, while D_5 is used as a tracer for personal care products. The correlation in these two tracers suggest that we not only measured the fumes from painting activities but likely also from personal care product emissions from the workers at the construction site. The aromatics in peak 2 may represent emissions from another activity occurring at the parking lot, or could be from another source, for example, a passing vehicle.

Because of flow smearing across the OFR (residence time of 1 min) and plumbing, we cannot apportion the observed OFR-produced OA between the sources that generated peaks 1 and 2. However, the time series in Figure 4a suggests that at least some of the enhanced SOA production at the parking lot is associated with the VCP-rich peak 1. Similarly, the SOA spike at the spray-painting site (Figure 4b) is associated with VCPs in peak 3.

Spikes of monoterpenes were observed at both the parking lot and spray painting sites. While the PTRMS cannot inform further detail about the type of MT (e.g., α-pinene versus limonene), a time-series-based approach can be used to distinguish MT contributions from VCPs (sudden peaks in time series due to highly local sources) versus biogenic (smoother change in time series while traversing from downtown to suburban green space). The MT increments shown in Figure 4 are thus likely also VCP influenced. Correlated increments of tracers, such as PCBTF and D_5, further reinforce the likelihood that the MTs are VCP-emitted.

Laboratory Experiments on SOA Formation Potential of VCPs. We investigated SOA potential of different VCPs in the laboratory. In these experiments, we injected a short (10−20 s) pulse of fumes from different VCPs into the OFR (Figure S12). Time series of gas- and particle-phase organics for the different VCPs are shown in Figure S13. The PTRMS data show substantial signal across a suite of organic gases at the OFR inlet. As the pulse travels through the OFR, there is a subsequent, smeared SOA response at the OFR outlet, measured by the AMS. The composition and magnitude of VCP emissions vary across different VCPs, and thus, the amount of SOA observed in the OFR also differs. For example, the oil-based paint fumes contained SOA precursors such as aromatics and MTs, whereas the sunblock lotion vapors did not contain any traditional SOA precursors. Yet, both sources produced SOA in the OFR. To quantify SOA potential, we normalized the SOA response (ΔOA = area under OA peak) to the acetone response (Δacetone). While acetone is not an SOA precursor, we used it as a proxy for precursors because it is a common component of VCP emissions across wide range of sources.[9] ΔOA/Δacetone, thus, gives a measure of the surrogate yield that we can compare across VCP mixtures. Instead of using just acetone, we also calculated a yield using the total response in all VOCs (Figure S14). Both forms of yields show orders-of-magnitude variation in the SOA potential, suggesting a wide range of both VCP composition and SOA formation potentials (Figure 5).

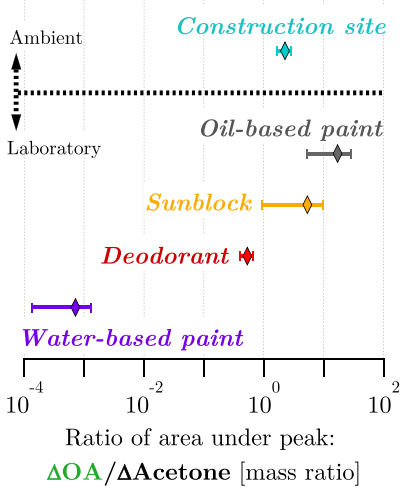

Figure 5. Ranked SOA potential of different VCPs tested in the lab, along with the SOA potential at the construction site. Note that the axis is logarithmically spaced. SOA potential is calculated by normalizing the amount of SOA formed in the OFR (i.e., area under peak in OA time-series; ΔOA) to the area under the peak in acetone time-series (Δacetone). While acetone is not an SOA precursor, we used it as a proxy for precursors because it is a common component of VCP emissions across wide range of sources.[9]

IMPLICATIONS OF THIS STUDY

We performed in situ oxidation of air in different urban environments and found that traditional (vehicular and biogenic) sources of SOA precursors do not fully explain the observed SOA potential. This finding is consistent with previous studies.[7,8,10] Our data further suggest that VCPs and other upstream sources (oil and gas extraction, coke ovens, etc.) can explain this additional SOA potential. While our in situ oxidation informs SOA potentials over long atmospheric time scales (~2 days), these differences in SOA potential also explain the previously reported intraurban and morning-afternoon differences in ambient SOA.[21]

DOI: 10.1021/acs.est.9b06531
Environ. Sci. Technol. XXXX, XXX, XXX−XXX

VCPs occur in a wide range of formulations, and thus exhibit a wide range of SOA potentials. Emissions from VCPs and upstream sources collectively account for 70% of the total emissions of petrochemical organic gases.[9] Our findings imply that these emissions also have significant contribution to SOA at the national level, and that characterization of their reactivity and SOA yield under different atmospherically relevant environmental conditions is warranted for achieving closure between modeled and observed urban aerosol levels, and for a better scientific understanding of human exposure to urban aerosols.

In addition to urban outdoor environments, our findings also have important implications for SOA formation in other types of environments: (a) sites of oil sands exploration, recently shown to be important upstream emission sources,[79,80] and global SOA sources,[79,81,82] and (b) indoor microenvironments, where strong oxidizing agents (typically O_3,[83] but sometimes also OH[84]) are present, and where VOC emissions are much higher than those outdoors.[9]

■ ASSOCIATED CONTENT

Supporting Information

The Supporting Information is available free of charge at https://pubs.acs.org/doi/10.1021/acs.est.9b06531.

Details on OFR calibration, operation, data analyses, and corrections; instrumentation details, measurement setup, and sampling locations; tracer-based estimation of HOA; details on speciated and source-based approach to SOA predictions; setup and instrumentation used for indoor VCP experiments; and detailed results about different VCPs, as well as expanded time series of VCP SOA observed at construction site (PDF)

■ AUTHOR INFORMATION

Corresponding Author

*E-mail: apresto@andrew.cmu.edu.

ORCID

Rishabh U. Shah: 0000-0002-4608-1972
Matthew M. Coggon: 0000-0002-5763-1925
Brian C. McDonald: 0000-0001-8600-5096
Allen L. Robinson: 0000-0002-1819-083X
Albert A. Presto: 0000-0002-9156-1094

Present Addresses

[¶]R.U.S.: Chemical Sciences Division, National Oceanic and Atmospheric Administration, Earth Systems Research Laboratory, Boulder CO, 80305.
[§]R.U.S.: Cooperative Institute for Research in Environmental Sciences, Boulder CO, 80309.

Notes

The authors declare no competing financial interest.

■ ACKNOWLEDGMENTS

We thank Fred Moshary and Mark Arend at City College of New York for assistance with sampling in Harlem. We thank Quanyang Lu and Provat Saha for helpful discussions. We acknowledge funding from two NSF projects (AGS1543786 and AGS1848324), a CIRES Innovative Research Proposal Grant, and NOAA grant NA17OAR4320101. We acknowledge project support from R J Lee Group, Inc. for providing their mobile laboratory equipped with the PTR-TOF-4000. This work is part of the Center for Air, Climate and Energy Solution (CACES). Funding was provided by the United States Environmental Protection Agency (assistance agreement no. RD83587301). *Disclaimer:* This work has not been formally reviewed by the funding agencies. The views expressed in this document are solely those of the authors and do not necessarily reflect those of the funding agencies. EPA does not endorse any products or commercial services mentioned in this publication.

■ REFERENCES

(1) Apte, J. S.; Marshall, J. D.; Cohen, A. J.; Brauer, M. Addressing Global Mortality from Ambient PM2.5. *Environ. Sci. Technol.* **2015**, *49*, 8057−8066.

(2) Myhre, G.; Samset, B. H.; Schulz, M.; Balkanski, Y.; Bauer, S.; Berntsen, T. K.; Bian, H.; Bellouin, N.; Chin, M.; Diehl, T.; Easter, R. C.; Feichter, J.; Ghan, S. J.; Hauglustaine, D.; Iversen, T.; Kinne, S.; Kirkevag, A.; Lamarque, J.-F.; Lin, G.; Liu, X.; Lund, M. T.; Luo, G.; Ma, X.; van Noije, T.; Penner, J. E.; Rasch, P. J.; Ruiz, A.; Seland, Ø.; Skeie, R. B.; Stier, P.; Takemura, T.; Tsigaridis, K.; Wang, P.; Wang, Z.; Xu, L.; Yu, H.; Yu, F.; Yoon, J.-H.; Zhang, K.; Zhang, H.; Zhou, C. Radiative forcing of the direct aerosol effect from AeroCom Phase II simulations. *Atmos. Chem. Phys.* **2013**, *13*, 1853−1877.

(3) Jimenez, J. L.; Canagaratna, M. R.; Donahue, N. M.; Prévôt, A. S. H.; Zhang, Q.; Kroll, J. H.; DeCarlo, P. F.; Allan, J. D.; Coe, H.; Ng, N. L.; Aiken, A. C.; Docherty, K. S.; Ulbrich, I. M.; Grieshop, A. P.; Robinson, A. L.; Duplissy, J.; Smith, J. D.; Wilson, K. R.; Lanz, V. A.; Hueglin, C.; Sun, Y. L.; Tian, J.; Laaksonen, A.; Raatikainen, T.; Rautiainen, J.; Vaattovaara, P.; Ehn, M.; Kulmala, M.; Tomlinson, J. M.; Collins, D. R.; Cubison, M. J.; Dunlea, E. J.; Huffman, J. A.; Onasch, T. B.; Alfarra, M. R.; Williams, P. I.; Bower, K.; Kondo, Y.; Schneider, J.; Drewnick, F.; Borrmann, S.; Weimer, S.; Demerjian, K.; Salcedo, D.; Cottrell, L.; Griffin, R.; Takami, A.; Miyoshi, T.; Hatakeyama, S.; Shimono, A.; Sun, J. Y.; Zhang, Y. M.; Dzepina, K.; Kimmel, J. R.; Sueper, D.; Jayne, J. T.; Herndon, S. C.; Trimborn, A. M.; Williams, L. R.; Wood, E. C.; Middlebrook, A. M.; Kolb, C. E.; Baltensperger, U.; Worsnop, D. R. Evolution of organic aerosols in the atmosphere. *Science* **2009**, *326*, 1525−1529.

(4) Zhang, Q.; Jimenez, J. L.; Canagaratna, M. R.; Allan, J. D.; Coe, H.; Ulbrich, I.; Al-farra, M. R.; Takami, A.; Middlebrook, A. M.; Sun, Y. L.; Dzepina, K.; Dunlea, E.; Docherty, K.; DeCarlo, P. F.; Salcedo, D.; Onasch, T.; Jayne, J. T.; Miyoshi, T.; Shimono, A.; Hatakeyama, S.; Takegawa, N.; Kondo, Y.; Schneider, J.; Drewnick, F.; Borrmann, S.; Weimer, S.; Demerjian, K.; Williams, P.; Bower, K.; Bahreini, R.; Cottrell, L.; Griffin, R. J.; Rautiainen, J.; Sun, J. Y.; Zhang, Y. M.; Worsnop, D. R. Ubiquity and dominance of oxygenated species in organic aerosols in anthropogenically-influenced Northern Hemisphere midlatitudes. *Geophys. Res. Lett.* **2007**, *34*, L13801.

(5) Mohr, C.; DeCarlo, P. F.; Heringa, M. F.; Chirico, R.; Richter, R.; Crippa, M.; Querol, X.; Baltensperger, U.; Prévôt, A. S. H. Spatial Variation of Aerosol Chemical Composition and Organic Components Identified by Positive Matrix Factorization in the Barcelona Region. *Environ. Sci. Technol.* **2015**, *49*, 10421−10430.

(6) Hildebrandt, L.; Engelhart, G. J.; Mohr, C.; Kostenidou, E.; Lanz, V. A.; Bougiatioti, A.; Decarlo, P. F.; Prévôt, A. S. H.; Baltensperger, U.; Mihalopoulos, N.; Donahue, N. M.; Pandis, S. N. Aged organic aerosol in the Eastern Mediterranean: The Finokalia Aerosol Measurement Experiment-2008. *Atmos. Chem. Phys.* **2010**, *10*, 4167−4186.

(7) Hodzic, A.; Jimenez, J. L.; Madronich, S.; Aiken, A. C.; Bessagnet, B.; Curci, G.; Fast, J.; Lamarque, J.-F.; Onasch, T. B.; Roux, G.; Schauer, J. J.; Stone, E. A.; Ulbrich, I. M. Modeling organic aerosols during MILAGRO: importance of biogenic secondary organic aerosols. *Atmos. Chem. Phys.* **2009**, *9*, 6949−6981.

(8) Hayes, P. L.; Carlton, A. G.; Baker, K. R.; Ahmadov, R.; Washenfelder, R. A.; Alvarez, S.; Rappenglück, B.; Gilman, J. B.; Kuster, W. C.; de Gouw, J. A.; Zotter, P.; Prévôt, A. S. H.; Szidat, S.; Kleindienst, T. E.; Offenberg, J. H.; Ma, P. K.; Jimenez, J. L. Modeling

DOI: 10.1021/acs.est.9b06531
Environ. Sci. Technol. XXXX, XXX, XXX−XXX

the formation and aging of secondary organic aerosols in Los Angeles during CalNex 2010. *Atmos. Chem. Phys.* **2015**, *15*, 5773−5801.
(9) McDonald, B. C.; De Gouw, J. A.; Gilman, J. B.; Jathar, S. H.; Akherati, A.; Cappa, C. D.; Jimenez, J. L.; Lee-Taylor, J.; Hayes, P. L.; McKeen, S. A.; Cui, Y. Y.; Kim, S. W.; Gentner, D. R.; Isaacman-VanWertz, G.; Goldstein, A. H.; Harley, R. A.; Frost, G. J.; Roberts, J. M.; Ryerson, T. B.; Trainer, M. Volatile chemical products emerging as largest petrochemical source of urban organic emissions. *Science* **2018**, *359*, 760−764.
(10) Akherati, A.; Cappa, C. D.; Kleeman, M. J.; Docherty, K. S.; Jimenez, J. L.; Griffith, S. M.; Dusanter, S.; Stevens, P. S.; Jathar, S. H. Simulating secondary organic aerosol in a regional air quality model using the statistical oxidation model - Part 3: Assessing the influence of semi-volatile and intermediate-volatility organic compounds and NO x. *Atmos. Chem. Phys.* **2019**, *19*, 4561−4594.
(11) Khare, P.; Gentner, D. R. Considering the future of anthropogenic gas-phase organic compound emissions and the increasing influence of non-combustion sources on urban air quality. *Atmos. Chem. Phys.* **2018**, *18*, 5391−5413.
(12) Zotter, P.; El-Haddad, I.; Zhang, Y.; Hayes, P. L.; Zhang, X.; Lin, Y.-H.; Wacker, L.; Schnelle-Kreis, J.; Abbaszade, G.; Zimmermann, R.; Surratt, J. D.; Weber, R.; Jimenez, J. L.; Szidat, S.; Baltensperger, U.; Prévôt, A. S. H. Diurnal cycle of fossil and nonfossil carbon using radiocarbon analyses during CalNex. *Journal of Geophysical Research: Atmospheres* **2014**, *119*, 6818−6835.
(13) Vlachou, A.; Daellenbach, K. R.; Bozzetti, C.; Chazeau, B.; Salazar, G. A.; Szidat, S.; Jaffrezo, J. L.; Hueglin, C.; Baltensperger, U.; El Haddad, I.; Prévôt, A. S. Advanced source apportionment of carbonaceous aerosols by coupling offline AMS and radiocarbon size-segregated measurements over a nearly 2-year period. *Atmos. Chem. Phys.* **2018**, *18*, 6187−6206.
(14) Janechek, N. J.; Marek, R. F.; Bryngelson, N.; Singh, A.; Bullard, R. L.; Brune, W. H.; Stanier, C. O. Physical properties of secondary photochemical aerosol from OH oxidation of a cyclic siloxane. *Atmos. Chem. Phys.* **2019**, *19*, 1649−1664.
(15) Kim, S. W.; McKeen, S. A.; Frost, G. J.; Lee, S. H.; Trainer, M.; Richter, A.; Angevine, W. M.; Atlas, E.; Bianco, L.; Boersma, K. F.; Brioude, J.; Burrows, J. P.; De Gouw, J.; Fried, A.; Gleason, J.; Hilboll, A.; Mellqvist, J.; Peischl, J.; Richter, D.; Rivera, C.; Ryerson, T.; Te Lintel Hekkert, S.; Walega, J.; Warneke, C.; Weibring, P.; Williams, E. Evaluations of NOx and highly reactive VOC emission inventories in Texas and their implications for ozone plume simulations during the Texas Air Quality Study 2006. *Atmos. Chem. Phys.* **2011**, *11*, 11361−11386.
(16) Ahmadov, R.; McKeen, S.; Trainer, M.; Banta, R.; Brewer, A.; Brown, S.; Edwards, P. M.; De Gouw, J. A.; Frost, G. J.; Gilman, J.; Helmig, D.; Johnson, B.; Karion, A.; Koss, A.; Langford, A.; Lerner, B.; Olson, J.; Oltmans, S.; Peischl, J.; Pétron, G.; Pichugina, Y.; Roberts, J. M.; Ryerson, T.; Schnell, R.; Senff, C.; Sweeney, C.; Thompson, C.; Veres, P. R.; Warneke, C.; Wild, R.; Williams, E. J.; Yuan, B.; Zamora, R. Understanding high wintertime ozone pollution events in an oil- and natural gas-producing region of the western US. *Atmos. Chem. Phys.* **2015**, *15*, 411−429.
(17) Easterly, T. W.; Shoup, S. P.; Kaegi, D. P. In *Metallurgical Coke: Air Pollution Engineering Manual*; Buonicore, A., Davis, W. T., Eds.; Van Nostrand Reinhold: New York, 1992.
(18) U.S. Environmental Protection Agency. *Emission Factor Documentation for AP-42*, 2008.
(19) U.S. Environmental Protection Agency. New Source Performance Standards, 2019. https://www.epa.gov/stationary-sources-air-pollution/new-source-performance-standards.
(20) U.S. Environmental Protection Agency. National Ambient Air Quality Standards, 2016. https://www.epa.gov/criteria-air-pollutants/naaqs-table.
(21) Shah, R. U.; Robinson, E. S.; Gu, P.; Robinson, A.; Apte, J. S.; Presto, A. A. Highspatial-resolution mapping and source apportionment of aerosol composition in Oakland, California using mobile aerosol mass spectrometry. *Atmos. Chem. Phys.* **2018**, *18*, 16325−16344.
(22) Gu, P.; Li, H. Z.; Ye, Q.; Robinson, E. S.; Apte, J. S.; Robinson, A. L.; Presto, A. A. Intracity variability of PM exposure is driven by carbonaceous sources and correlated with land use variables. *Environ. Sci. Technol.* **2018**, *52*, 11545−11554, DOI: 10.1021/acs.est.8b03833.
(23) Coggon, M. M.; McDonald, B. C.; Vlasenko, A.; Veres, P. R.; Bernard, F.; Koss, A. R.; Yuan, B.; Gilman, J. B.; Peischl, J.; Aikin, K. C.; DuRant, J.; Warneke, C.; Li, S.-m.; de Gouw, J. A. Diurnal Variability and Emission Pattern of Decamethylcyclopentasiloxane (D 5) from the Application of Personal Care Products in Two North American Cities. *Environ. Sci. Technol.* **2018**, *52*, 5610−5618.
(24) Fujita, E. M.; Campbell, D. E.; Patrick Arnott, W.; Lau, V.; Martien, P. T. Spatial variations of particulate matter and air toxics in communities adjacent to the Port of Oakland. *J. Air Waste Manage. Assoc.* **2013**, *63*, 1399−1411.
(25) Weitkamp, E. A.; Lipsky, E. M.; Pancras, P. J.; Ondov, J. M.; Polidori, A.; Turpin, B. J.; Robinson, A. L. Fine particle emission profile for a large coke production facility based on highly time-resolved fence line measurements. *Atmos. Environ.* **2005**, *39*, 6719−6733.
(26) ACHD. *Point Source Emission Inventory Report 2011*, 2011.
(27) Gu, P.; Dallmann, T. R.; Li, H. Z.; Tan, Y.; Presto, A. A. Quantifying urban spatial variations of anthropogenic VOC concentrations and source contributions with a mobile sampling platform. *Int. J. Environ. Res. Public Health* **2019**, *16*, 1632.
(28) Yuan, B.; Koss, A.; Warneke, C.; Gilman, J. B.; Lerner, B. M.; Stark, H.; De Gouw, J. A. A high-resolution time-of-flight chemical ionization mass spectrometer utilizing hydronium ions (H3O+ToF-CIMS) for measurements of volatile organic compounds in the atmosphere. *Atmos. Meas. Tech.* **2016**, *9*, 2735−2752.
(29) Saha, P. K.; Reece, S. M.; Grieshop, A. P. Seasonally Varying Secondary Organic Aerosol Formation from In-Situ Oxidation of Near-Highway Air. *Environ. Sci. Technol.* **2018**, *52*, 7192−7202.
(30) Palm, B. B.; de Sa, S. S.; Day, D. A.; Campuzano-Jost, P.; Hu, W.; Seco, R.; Sjostedt, S. J.; Park, J.-H.; Guenther, A. B.; Kim, S.; Brito, J.; Wurm, F.; Artaxo, P.; Thalman, R.; Wang, J.; Yee, L. D.; Wernis, R.; Isaacman-VanWertz, G.; Goldstein, A. H.; Liu, Y.; Springston, S. R.; Souza, R.; Newburn, M. K.; Alexander, M. L.; Martin, S. T.; Jimenez, J. L. Secondary organic aerosol formation from ambient air in an oxidation flow reactor in central Amazonia. *Atmos. Chem. Phys.* **2018**, *18*, 467−493.
(31) Peng, Z.; Day, D. A.; Ortega, A. M.; Palm, B. B.; Hu, W.; Stark, H.; Li, R.; Tsigaridis, K.; Brune, W. H.; Jimenez, J. L. Non-OH chemistry in oxidation flow reactors for the study of atmospheric chemistry systematically examined by modeling. *Atmos. Chem. Phys.* **2016**, *16*, 4283−4305.
(32) Mao, J.; Ren, X.; Brune, W. H.; Olson, J. R.; Crawford, J. H.; Fried, A.; Huey, L. G.; Cohen, R. C.; Heikes, B.; Singh, H. B.; Blake, D. R.; Sachse, G. W.; Diskin, G. S.; Hall, S. R.; Shetter, R. E. Airborne measurement of OH reactivity during INTEX-B. *Atmos. Chem. Phys.* **2009**, *9*, 163−173.
(33) Palm, B. B.; Campuzano-Jost, P.; Ortega, A. M.; Day, D. A.; Kaser, L.; Jud, W.; Karl, T.; Hansel, A.; Hunter, J. F.; Cross, E. S.; Kroll, J. H.; Peng, Z.; Brune, W. H.; Jimenez, J. L. In situ secondary organic aerosol formation from ambient pine forest air using an oxidation flow reactor. *Atmos. Chem. Phys.* **2016**, *16*, 2943−2970.
(34) Sueper, D.; Allan, J. D.; Dunlea, E.; Crosier, J.; Kimmel, J. R.; DeCarlo, P. F.; Aiken, A. C.; Jimenez, J. L. *A Community Software for Quality Control and Analysis of Data from the Aerodyne Time-of-Flight Aerosol Mass Spectrometers (ToF-AMS)*, 2007.
(35) Middlebrook, A. M.; Bahreini, R.; Jimenez, J. L.; Canagaratna, M. R. Evaluation of Composition-Dependent Collection Efficiencies for the Aerodyne Aerosol Mass Spectrometer using Field Data. *Aerosol Sci. Technol.* **2012**, *46*, 258−271.
(36) Mohr, C.; DeCarlo, P. F.; Heringa, M. F.; Chirico, R.; Slowik, J. G.; Richter, R.; Reche, C.; Alastuey, A.; Querol, X.; Seco, R.; Peñuelas, J.; Jiménez, J. L.; Crippa, M.; Zimmermann, R.; Baltensperger, U.; Prévôt, A. S. H. Identification and quantification of organic aerosol from cooking and other sources in Barcelona using

aerosol mass spectrometer data. *Atmos. Chem. Phys.* **2012**, *12*, 1649−1665.
(37) Ng, N. L.; Canagaratna, M. R.; Jimenez, J. L.; Zhang, Q.; Ulbrich, I. M.; Worsnop, D. R. Real-time methods for estimating organic component mass concentrations from aerosol mass spectrometer data. *Environ. Sci. Technol.* **2011**, *45*, 910−916.
(38) Donahue, N. M.; Epstein, S. A.; Pandis, S. N.; Robinson, A. L. A two-dimensional volatility basis set: 1. organic-aerosol mixing thermodynamics. *Atmos. Chem. Phys.* **2011**, *11*, 3303−3318.
(39) Donahue, N. M.; Kroll, J. H.; Pandis, S. N.; Robinson, A. L. A two-dimensional volatility basis set-Part 2: Diagnostics of organic-aerosol evolution. *Atmos. Chem. Phys.* **2012**, *12*, 615−634.
(40) Erickson, M. H.; Gueneron, M.; Jobson, B. T. Measuring long chain alkanes in diesel engine exhaust by thermal desorption PTR-MS. *Atmos. Meas. Tech.* **2014**, *7*, 225−239.
(41) Liu, X.; Deming, B.; Pagonis, D.; Day, D. A.; Palm, B. B.; Talukdar, R.; Roberts, J. M.; Veres, P. R.; Krechmer, J. E.; Thornton, J. A.; De Gouw, J. A.; Ziemann, P. J.; Jimenez, J. L. Effects of gas-wall interactions on measurements of semivolatile compounds and small polar molecules. *Atmos. Meas. Tech.* **2019**, *12*, 3137−3149.
(42) Deming, B.; Pagonis, D.; Liu, X.; Day, D.; Talukdar, R.; Krechmer, J.; de Gouw, J. A.; Jimenez, J. L.; Ziemann, P. J. Measurements of Delays of Gas-Phase Compounds in a Wide Variety of Tubing Materials due to Gas-Wall Interactions. *Atmos. Meas. Tech.* **2019**, *12*, 3453−3461.
(43) Tkacik, D. S.; Presto, A. A.; Donahue, N. M.; Robinson, A. L. Secondary organic aerosol formation from intermediate-volatility organic compounds: Cyclic, linear, and branched alkanes. *Environ. Sci. Technol.* **2012**, *46*, 8773−8781.
(44) Zhao, Y.; Hennigan, C. J.; May, A. A.; Tkacik, D. S.; De Gouw, J. A.; Gilman, J. B.; Kuster, W. C.; Borbon, A.; Robinson, A. L. Intermediate-volatility organic compounds: A large source of secondary organic aerosol. *Environ. Sci. Technol.* **2014**, *48*, 13743−13750.
(45) Ortega, A. M.; Hayes, P. L.; Peng, Z.; Palm, B. B.; Hu, W.; Day, D. A.; Li, R.; Cubison, M. J.; Brune, W. H.; Graus, M.; Warneke, C.; Gilman, J. B.; Kuster, W. C.; De Gouw, J.; Gutiérrez-Montes, C.; Jimenez, J. L. Real-time measurements of secondary organic aerosol formation and aging from ambient air in an oxidation flow reactor in the Los Angeles area. *Atmos. Chem. Phys.* **2016**, *16*, 7411−7433.
(46) Zhao, Y.; Nguyen, N. T.; Presto, A. A.; Hennigan, C. J.; May, A. A.; Robinson, A. L. Intermediate Volatility Organic Compound Emissions from On-Road Diesel Vehicles: Chemical Composition, Emission Factors, and Estimated Secondary Organic Aerosol Production. *Environ. Sci. Technol.* **2015**, *49*, 11516−11526.
(47) Zhao, Y.; Nguyen, N. T.; Presto, A. A.; Hennigan, C. J.; May, A. A.; Robinson, A. L. Intermediate Volatility Organic Compound Emissions from On-Road Gasoline Vehicles and Small Off-Road Gasoline Engines. *Environ. Sci. Technol.* **2016**, *50*, 4554−4563.
(48) Lu, Q.; Zhao, Y.; Robinson, A. L. Comprehensive organic emission profiles for gasoline, diesel, and gas-turbine engines including intermediate and semi-volatile organic compound emissions. *Atmos. Chem. Phys.* **2018**, *18*, 17637−17654.
(49) Nault, B. A.; Campuzano-Jost, P.; Day, D. A.; Schroder, J. C.; Anderson, B.; Beyersdorf, A. J.; Blake, D. R.; Brune, W. H.; Choi, Y.; Corr, C. A.; de Gouw, J. A.; Dibb, J.; DiGangi, J. P.; Diskin, G. S.; Fried, A.; Huey, L. G.; Kim, M. J.; Knote, C. J.; Lamb, K. D.; Lee, T.; Park, T.; Pusede, S. E.; Scheuer, E.; Thornhill, K. L.; Woo, J.-H.; Jimenez, J. L. Secondary organic aerosol production from local emissions dominates the organic aerosol budget over Seoul, South Korea, during KORUS-AQ. *Atmos. Chem. Phys.* **2018**, *18*, 17769−17800.
(50) Jathar, S. H.; Gordon, T. D.; Hennigan, C. J.; Pye, H. O. T.; Pouliot, G.; Adams, P. J.; Donahue, N. M.; Robinson, A. L. Unspeciated organic emissions from combustion sources and their influence on the secondary organic aerosol budget in the United States. *Proc. Natl. Acad. Sci. U. S. A.* **2014**, *111*, 10473−10478.
(51) Tkacik, D. S.; Lambe, A. T.; Jathar, S.; Li, X.; Presto, A. A.; Zhao, Y.; Blake, D. R.; Meinardi, S.; Jayne, J. T.; Croteau, P. L.; Robinson, A. L. Secondary Organic Aerosol Formation from in-Use Motor Vehicle Emissions Using a Potential Aerosol Mass Reactor. *Environ. Sci. Technol.* **2014**, *48*, 11235−11242.
(52) Lambe, A. T.; Chhabra, P. S.; Onasch, T. B.; Brune, W. H.; Hunter, J. F.; Kroll, J. H.; Cummings, M. J.; Brogan, J. F.; Parmar, Y.; Worsnop, D. R.; Kolb, C. E.; Davidovits, P. Effect of oxidant concentration, exposure time, and seed particles on secondary organic aerosol chemical composition and yield. *Atmos. Chem. Phys.* **2015**, *15*, 3063−3075.
(53) Lane, T. E.; Donahue, N. M.; Pandis, S. N. Simulating secondary organic aerosol formation using the volatility basis-set approach in a chemical transport model. *Atmos. Environ.* **2008**, *42*, 7439−7451.
(54) Sun, Y. L.; Zhang, Q.; Schwab, J. J.; Demerjian, K. L.; Chen, W. N.; Bae, M. S.; Hung, H. M.; Hogrefe, O.; Frank, B.; Rattigan, O. V.; Lin, Y. C. Characterization of the sources and processes of organic and inorganic aerosols in New York city with a high-resolution time-of-flight aerosol mass apectrometer. *Atmos. Chem. Phys.* **2011**, *11*, 1581−1602.
(55) Hayes, P. L.; Ortega, A. M.; Cubison, M. J.; Froyd, K. D.; Zhao, Y.; Cliff, S. S.; Hu, W. W.; Toohey, D. W.; Flynn, J. H.; Lefer, B. L.; Grossberg, N.; Alvarez, S.; Rappenglück, B.; Taylor, J. W.; Allan, J. D.; Holloway, J. S.; Gilman, J. B.; Kuster, W. C.; De Gouw, J. A.; Massoli, P.; Zhang, X.; Liu, J.; Weber, R. J.; Corrigan, A. L.; Russell, L. M.; Isaacman, G.; Worton, D. R.; Kreisberg, N. M.; Goldstein, A. H.; Thalman, R.; Waxman, E. M.; Volkamer, R.; Lin, Y. H.; Surratt, J. D.; Kleindienst, T. E.; Offenberg, J. H.; Dusanter, S.; Griffith, S.; Stevens, P. S.; Brioude, J.; Angevine, W. M.; Jimenez, J. L. Organic aerosol composition and sources in Pasadena, California, during the 2010 CalNex campaign. *Journal of Geophysical Research Atmospheres* **2013**, *118*, 9233−9257.
(56) Bahreini, R.; Ahmadov, R.; McKeen, S. A.; Vu, K. T.; Dingle, J. H.; Apel, E. C.; Blake, D. R.; Blake, N.; Campos, T. L.; Cantrell, C.; Flocke, F.; Fried, A.; Gilman, J. B.; Hills, A. J.; Hornbrook, R. S.; Huey, G.; Kaser, L.; Lerner, B. M.; Mauldin, R. L.; Meinardi, S.; Montzka, D. D.; Richter, D.; Schroeder, J. R.; Stell, M.; Tanner, D.; Walega, J.; Weibring, P.; Weinheimer, A. Sources and characteristics of summertime organic aerosol in the Colorado Front Range: Perspective from measurements and WRF-Chem modeling. *Atmos. Chem. Phys.* **2018**, *18*, 8293−8312.
(57) Tunno, B. J.; Dalton, R.; Michanowicz, D. R.; Shmool, J. L.; Kinnee, E.; Tripathy, S.; Cambal, L.; Clougherty, J. E. Spatial patterning in PM2.5 constituents under an inversion-focused sampling design across an urban area of complex terrain. *J. Exposure Sci. Environ. Epidemiol.* **2016**, *26*, 385−396.
(58) Katsoulis, B. D. Some meteorological aspects of air pollution in Athens, Greece. *Meteorology and Atmospheric Physics* **1988**, *39*, 203−212.
(59) Anquetin, S.; Guilbaud, C.; Chollet, J. P. Thermal valley inversion impact on the dispersion of a passive pollutant in a complex mountainous area. *Atmos. Environ.* **1999**, *33*, 3953−3959.
(60) Wallace, J.; Corr, D.; Kanaroglou, P. Topographic and spatial impacts of temperature inversions on air quality using mobile air pollution surveys. *Sci. Total Environ.* **2010**, *408*, 5086−5096.
(61) Logue, J. M.; Huff-Hartz, K. E.; Lambe, A. T.; Donahue, N. M.; Robinson, A. L. High time-resolved measurements of organic air toxics in different source regimes. *Atmos. Environ.* **2009**, *43*, 6205−6217.
(62) Gill, K. J.; Hites, R. A. Rate Constants for the Gas-Phase Reactions of the Hydroxyl Radical with Isoprene, $\alpha$and β-Pinene, and Limonene as a Function of Temperature. *J. Phys. Chem. A* **2002**, *106*, 2538−2544.
(63) Singer, B. C.; Destaillats, H.; Hodgson, A. T.; Nazaroff, W. W. Cleaning products and air fresheners: Emissions and resulting concentrations of glycol ethers and terpenoids. *Indoor Air* **2006**, *16*, 179−191.
(64) Li, K.; Li, J.; Tong, S.; Wang, W.; Huang, R.-J.; Ge, M. Characteristics of wintertime VOCs in suburban and urban Beijing:

DOI: 10.1021/acs.est.9b06531
Environ. Sci. Technol. XXXX, XXX, XXX−XXX

concentrations, emission ratios, and festival effects. *Atmos. Chem. Phys.* **2019**, *19*, 8021−8036.
(65) Lee, E. G.; Lewis, B.; Burns, D. A.; Kashon, M. L.; Kim, S. W.; Harper, M. Assessing Exposures to 1-chloro-4-(trifluoromethyl) Benzene (PCBTF) in U.S. Workplaces. *J. Occup. Environ. Hyg.* **2015**, *12*, D123−D130.
(66) Harley, R. A.; Hannigan, M. P.; Cass, G. R. Respeciation of Organic Gas Emissions and the Detection of Excess Unburned Gasoline in the Atmosphere. *Environ. Sci. Technol.* **1992**, *26*, 2395−2408.
(67) Li, W.; Li, L.; Chen, C.-l.; Kacarab, M.; Peng, W.; Price, D.; Xu, J.; Cocker, D. R. Potential of select intermediate-volatility organic compounds and consumer products for secondary organic aerosol and ozone formation under relevant urban conditions. *Atmos. Environ.* **2018**, *178*, 109−117.
(68) Palm, B. B.; Campuzano-Jost, P.; Day, D. A.; Ortega, A. M.; Fry, J. L.; Brown, S. S.; Zarzana, K. J.; Dube, W.; Wagner, N. L.; Draper, D. C.; Kaser, L.; Jud, W.; Karl, T.; Hansel, A.; Gutiérrez-Montes, C.; Jimenez, J. L. Secondary organic aerosol formation from in situ OH, O3, and NO3 oxidation of ambient forest air in an oxidation flow reactor. *Atmos. Chem. Phys.* **2017**, *17*, 5331−5354.
(69) Borbon, A.; Gilman, J. B.; Kuster, W. C.; Grand, N.; Chevaillier, S.; Colomb, A.; Dolgorouky, C.; Gros, V.; Lopez, M.; Sarda-Esteve, R.; Holloway, J.; Stutz, J.; Petetin, H.; McKeen, S.; Beekmann, M.; Warneke, C.; Parrish, D. D.; De Gouw, J. A. Emission ratios of anthropogenic volatile organic compounds in northern mid-latitude megacities: Observations versus emission inventories in Los Angeles and Paris. *Journal of Geophysical Research Atmospheres* **2013**, *118*, 2041−2057.
(70) Robinson, E. S.; Gu, P.; Ye, Q.; Li, H. Z.; Shah, R. U.; Apte, J. S.; Robinson, A. L.; Presto, A. A. Restaurant Impacts on Outdoor Air Quality: Elevated Organic Aerosol Mass from Restaurant Cooking with Neighborhood-Scale Plume Extents. *Environ. Sci. Technol.* **2018**, *52*, 9285−9294.
(71) Robinson, E. S.; Shah, R. U.; Messier, K.; Gu, P.; Li, H. Z.; Apte, J. S.; Robinson, A. L.; Presto, A. A. Land-Use Regression Modeling of Source-Resolved Fine Particulate Matter Components from Mobile Sampling. *Environ. Sci. Technol.* **2019**, *53*, 8925−8937.
(72) Li, Y.; Tasoglou, A.; Liangou, A.; Cain, K. P.; Jahn, L.; Gu, P.; Kostenidou, E.; Pandis, S. N. Cloud condensation nuclei activity and hygroscopicity of fresh and aged cooking organic aerosol. *Atmos. Environ.* **2018**, *176*, 103−109.
(73) Kaltsonoudis, C.; Kostenidou, E.; Louvaris, E.; Psichoudaki, M.; Tsiligiannis, E.; Florou, K.; Liangou, A.; Pandis, S. N. Characterization of fresh and aged organic aerosol emissions from meat charbroiling. *Atmos. Chem. Phys.* **2017**, *17*, 7143−7155.
(74) Liu, T.; Zhou, L.; LIU, Q.; Lee, B. P.; Yao, D.; Lu, H.; Lyu, X.; Guo, H.; Chan, C. K. Secondary Organic Aerosol Formation from Urban Roadside Air in Hong Kong. *Environ. Sci. Technol.* **2019**, *53*, 3001−3009.
(75) Liu, T.; Wang, Z.; Wang, X.; Chan, C. K. Primary and secondary organic aerosol from heated cooking oil emissions. *Atmos. Chem. Phys.* **2018**, *18*, 11363−11374.
(76) Zhang, X.; Cappa, C. D.; Jathar, S. H.; McVay, R. C.; Ensberg, J. J.; Kleeman, M. J.; Seinfeld, J. H. Influence of vapor wall loss in laboratory chambers on yields of secondary organic aerosol. *Proc. Natl. Acad. Sci. U. S. A.* **2014**, *111*, 5802−5807.
(77) Ng, N. L.; Kroll, J. H.; Chan, A. W.; Chhabra, P. S.; Flagan, R. C.; Seinfeld, J. H. Secondary organic aerosol formation from m-xylene, toluene, and benzene. *Atmos. Chem. Phys.* **2007**, *7*, 3909−3922.
(78) Drozd, G. T.; Zhao, Y.; Saliba, G.; Frodin, B.; Maddox, C.; Oliver Chang, M. C.; Maldonado, H.; Sardar, S.; Weber, R. J.; Robinson, A. L.; Goldstein, A. H. Detailed Speciation of Intermediate Volatility and Semivolatile Organic Compound Emissions from Gasoline Vehicles: Effects of Cold-Starts and Implications for Secondary Organic Aerosol Formation. *Environ. Sci. Technol.* **2019**, *53*, 1706−1714.
(79) Li, R.; Palm, B. B.; Borbon, A.; Graus, M.; Warneke, C.; Ortega, A. M.; Day, D. A.; Brune, W. H.; Jimenez, J. L.; De Gouw, J. A. Laboratory studies on secondary organic aerosol formation from crude oil vapors. *Environ. Sci. Technol.* **2013**, *47*, 12566−12574.
(80) Simpson, I. J.; Blake, N. J.; Barletta, B.; Diskin, G. S.; Fuelberg, H. E.; Gorham, K.; Huey, L. G.; Meinardi, S.; Rowland, F. S.; Vay, S. A.; Weinheimer, A. J.; Yang, M.; Blake, D. R. Characterization of trace gases measured over alberta oil sands mining operations: 76 speciated C2-C10 volatile organic compounds (VOCs), CO2, CH4, CO, NO, NO2, NOy, O3 and SO2. *Atmos. Chem. Phys.* **2010**, *10*, 11931−11954.
(81) Liggio, J.; Li, S. M.; Hayden, K.; Taha, Y. M.; Stroud, C.; Darlington, A.; Drollette, B. D.; Gordon, M.; Lee, P.; Liu, P.; Leithead, A.; Moussa, S. G.; Wang, D.; O'Brien, J.; Mittermeier, R. L.; Brook, J. R.; Lu, G.; Staebler, R. M.; Han, Y.; Tokarek, T. W.; Osthoff, H. D.; Makar, P. A.; Zhang, J.; Plata, D. L.; Gentner, D. R. Oil sands operations as a large source of secondary organic aerosols. *Nature* **2016**, *534*, 91−94.
(82) Liu, Q.; Shahpoury, P.; Liggio, J.; Harner, T.; Li, K.; Lee, P.; Li, S.-M. Understanding the Impact of High-NOx Conditions on the Formation of Secondary Organic Aerosol in the Photooxidation of Oil Sand-Related Precursors. *Environ. Sci. Technol. Lett.* **2019**, DOI: 10.1021/acs.estlett.9b00700.
(83) Weschler, C. J.; Carslaw, N. Indoor Chemistry. *Environ. Sci. Technol.* **2018**, *52*, 2419−2428.
(84) Gomez Alvarez, E.; Amedro, D.; Afif, C.; Gligorovski, S.; Schoemaecker, C.; Fittschen, C.; Doussin, J.-F.; Wortham, H. Unexpectedly high indoor hydroxyl radical concentrations associated with nitrous acid. *Proc. Natl. Acad. Sci. U. S. A.* **2013**, *110*, 13294−13299.

DOI: 10.1021/acs.est.9b06531
Environ. Sci. Technol. XXXX, XXX, XXX−XXX